EurJOC
European Journal of Organic Chemistry

A Journal of ChemPubSoc Europe

Accepted Article

Title: Quinoidization of π-Expanded Aromatic Diimides: Photophysics, Aromaticity, and Stability of the Novel Quinoidal Acenes

Authors: Nareshbabu Kamatham, Jingbai Li, Siamak Shokri, Guang Yang, Steffen Jockusch, Andrey Yu Rogachev, and Anoklase Jean-Luc Ayitou

To be cited as: *Eur. J. Org. Chem.* 10.1002/ejoc.201901456

Link to VoR: http://dx.doi.org/10.1002/ejoc.201901456

Supported by ACES Asian Chemical Editorial Society

WILEY-VCH

WILEY-VCH

COMMUNICATION

Quinoidization of π-Expanded Aromatic Diimides: Photophysics, Aromaticity, and Stability of the Novel Quinoidal Acenes

Nareshbabu Kamatham,[a] Jingbai Li,[a] Siamak Shokri,[a] Guang Yang,[a] Steffen Jockusch,[b] Andrey Yu. Rogachev*[a] and A. Jean-Luc Ayitou*[a]

Abstract: We report the synthesis and photophysical characterization of π-expanded quinoidal triplet chromophores which exhibits attractive light-harvesting properties. The kinetic of the triplet excited state of quinoidal benzotetraphene **2** was found to be one order of magnitude higher than the lifetime of ^{3}(**1**)* from the less conjugated parent chromophore **1**. Furthermore, the evaluation of the optoelectronic properties indicates that π-expansion helps narrow the optoelectronic bandgap; but, the influence of the additional aromatic rings in the structure of **2** and **3** compromises the stability of the *p*–quinoidal ring. QDM **2** was isolated and fully characterized; but, it was found to rearomatize to a mixture of uncharacterized radical species.

Introduction

Polyaromatic rylene and acene chromophores are actively researched owing to their attractive light-harvesting properties and tunable optoelectronic bandgap, which dictates excitons dynamics and kinetics in organic photonic materials/devices.[1-4] Undeniably, the behavior, photo-kinetics, and stability of the corresponding excited polyaromatic systems are essential to the modulation and transformation of absorbed radiation in many photonic materials. In recent years, significant contributions aiming to alter the excited state behaviors and/or properties of polyaromatic chromophores have been disseminated in the chemical literature.[5-11] Yet, there is more room at the bottom to explore other variables and factors that can be employed to tune the photophysics of these chromophores. A known strategy that allows to tune the photo-kinetics of polyaromatics relies on perturbing the intrinsic ground state aromaticity by inserting pro/non-aromatic units such as *para*-quinodimethyl ring (*p*-QDM) in the backbone of organic polyaromatics with the expectation to generate metastable triplet excited species via aromaticity reversal.[13-14]

We recently demonstrated that the fusion of a *p*-QDM unit to a phenylene ring can generate a new naphthoquinodimethane chromophore **1** (Figure 1) which exhibits unusual ground and excited state aromaticity and photophysical properties.[13] Our previously reported quinoidal chromophore can also be employed as a light-harvesting triplet sensitizer for photonic research such as triplet-triplet annihilation photon upconversion.[14] From the previous report, we showcased a new cycloaddition reaction of π-acidic diimides in the presence of phosphine disulfide, as Lawesson's reagent, to afford QDM **1**. Inspired by the earlier success to convert readily available naphthalene diimides to the corresponding triplet sensitizer by modulating the intrinsic aromaticity of the π–core, we wish to extend the new cycloaddition reaction to other π–expanded acene diimides[15-18] to afford novel quinoidal acene triplet sensitizers quinoidal benzotetraphene **2** and its thiophene analog **3** (Figure 1). Unexpectedly, quinoidal thiophene **3** decomposes during purification.

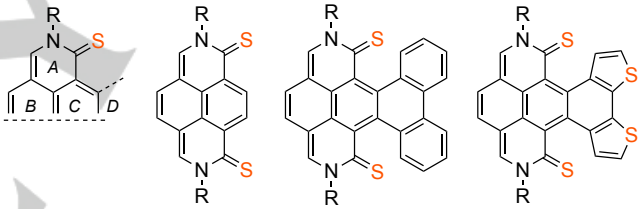

Figure 1. Chemical structures of QDM **1**–**3**: R = *n*–C_8H_{17}.

Results and Discussion

In the present investigation, we are particularly interested to red-shift the absorption band of QDM **1** using the π–expansion synthetic strategy. With this in mind, we hoped to isolate the new QDM derivatives **2** and **3** which were proposed to absorb red photons. The synthetic route leading to QDM **2** is depicted in Scheme 1 (See Experimental Section & Supplementary Information for the synthesis of diimide precursor to QDM **3**). Using well-documented procedures, we first converted naphthalene dianhydride (**NDA**) to the corresponding brominated NDA (**Br–NDA** and **Br$_2$–NDA**) using dibromoisocyanuric acid. Next, the combined brominated **NDA** was reacted with *n*-octylamine to afford **Br–NDI** in quantitative yield after separation/purification. The monobrominated NDI was reacted with bis-tributyltin to afford the corresponding stannated NDI (**Sn–NDI**) following a reported procedure.[19] Under Stille coupling conditions, **Sn–NDI** and 2,2'–dibromophenyl were reacted in refluxing Argon saturated toluene solution in the presence of catalytic amount of $Pd(PPh_3)_4$ for 12 h. As reported by Yue *et. al.*,[19] Stille coupling reaction will also induce a sp^2C–H activation to afford the expected annulated π-expanded diimide.

[a] Dr. Nareshbabu Kamatham, Dr. Jingbai Li, Dr. Siamak Shokri, Guang Yang, Prof. Andrey Yu Rogachev, Prof. A. Jean-Luc Ayitou
Department of Chemistry
Illinois Institute of Technology
3101 S Dearborn St.
Chicago, IL 60616 USA
E-mail: arogache@iit.edu and aayitou@iit.edu
[b] Dr. Steffen Jockusch
Department of Chemistry
Columbia University
New York, NY 10027 USA

Benzotetraphene diimide (**BTDI**) was isolated in 38% yield and was further used in the Lawesson-reagent-mediated quinoidization reaction to obtain the expected QDM **2** in 22 % yield as depicted in Scheme 1. A more detailed synthetic procedure for all compounds in Scheme 1 is also reported in the Experimental Section and Supplementary Information (Scheme S1). QDM **2** was characterized by NMR, UV-vis and FTIR spectroscopy methods (Supplementary Information).

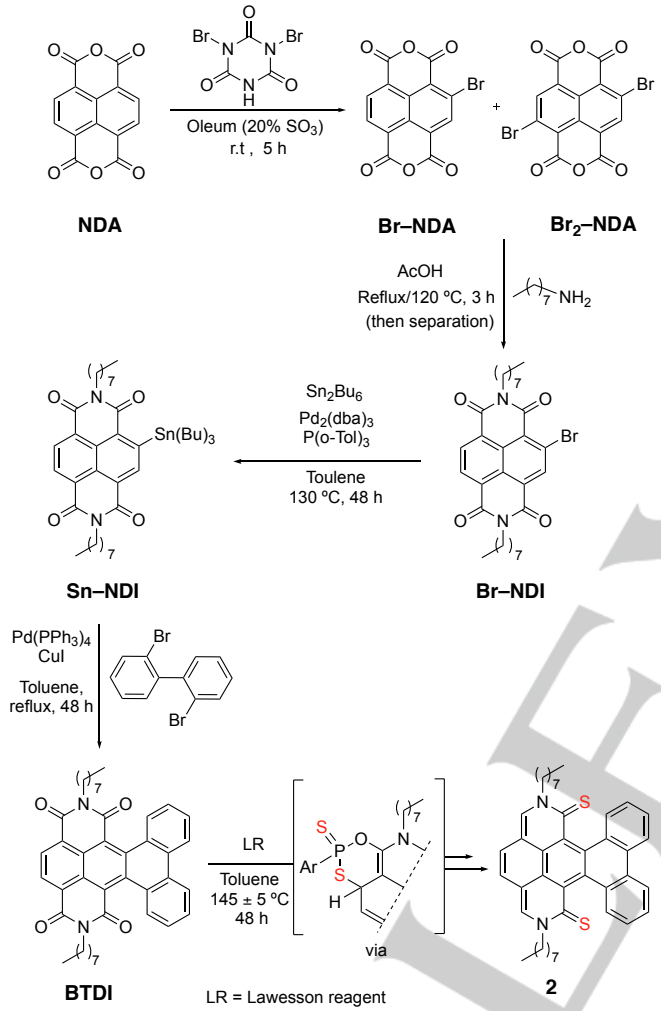

Scheme 1. Synthesis scheme for QDM **2**.

For the reaction depicted in Scheme 1, we hypothesize that the reaction pathway leading to QDM **2** (and **3**) could also produce the thermodynamic regio-isomers, where the thiocarbonyl groups are outside the fjord of the π-expansion: a comprehensive mechanistic rationale is depicted in the Supplementary Information (Figure S18). Nonetheless, on the basis of our previously reported mechanistic rationale (for QDM **1**)[13] and additional computational data, it was found that the pathway to form the doubly de-aromatized phosphinine intermediate(s) that would lead to the regio-isomers of **2** (and **3**) is kinetically not favored.

After isolating the expected quinoidal benzotetraphene **2,** its UV−vis absorption and emission profiles were recorded and compared to the ones of the parent structure **1**. As shown in Figure 2a, the absorption profile of QDM **2** is ca. 20 nm red-shifted, but exhibits a decrease of ca. 200 M^{-1} cm^{-1} in molar absorptivity at λ_{max} (Table 1). The slight red-shift in absorption is indicative of the additional π-conjugation, which also helps decrease the HOMO–LUMO gap from 3.18 to 2.95 eV (Figure 4 & Table 1). Also shown in Figure 2b are the steady state and matrix isolated emission bands of QDM **2**, which again showcase similar vibronic features similar to the ones seen in the emission bands of parent QDM **1**. Nonetheless, one can see that there is a ca. 15 nm shift in both the fluorescence and phosphorescence bands which is indicative of the presence of π-expanded core in QDM **2**. We then measured the phosphorescence decay kinetics of the two compounds to ascertain the effect of π-expansion on the kinetics of their corresponding aromatic triplet species. As shown in Figure 2c, the lowest triplet excited state of QDM **2** gave a lifetime value of 4.4 ms (Figure 2c, Table 1). This value is one order of magnitude higher than the lifetime of ^{3}(**1**)* indicating a likely change/increase in aromaticity of the quinoidal *ring B* of QDM **2**. We had previously hypothesized aromaticity reversal of QDM molecules in the excited states; in the case of QDM **2**, one can see that the additional two Clar's sextets (from the phenanthro unit) is mostly likely contributing in the stabilization of the triplet excited state in comparison to the effect of only one Clar's sextet: (See Chart S2, Supplementary Information for the corresponding resonance structures).

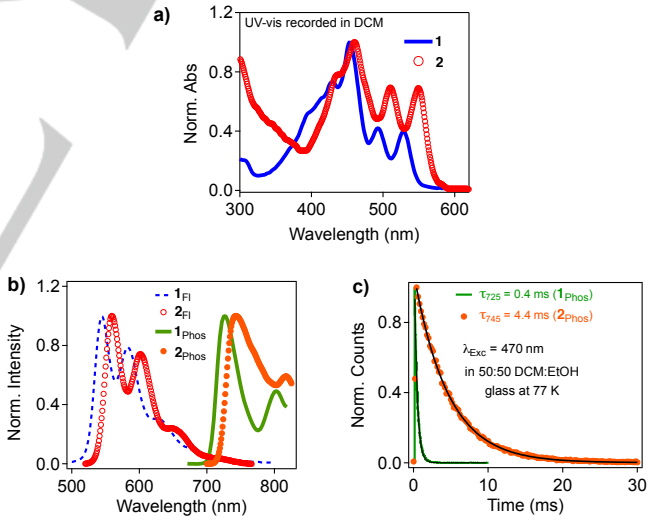

Figure 2. a) Normalized UV-Vis absorption spectra of QDM **1** and **2** recorded in dichloromethane (DCM). b) Steady state (fluorescence) and phosphorescence emission bands in DCM and 50:50 DCM:EtOH glass at 77 K, respectively, of QDM **1** and **2** (samples OD = 0.1 at λ_{Exc} = 470 nm). c) Phosphorescence decay kinetic of QDM **1** and **2** recorded in 50:50 DCM:EtOH glass at 77 K. Phosphorescence emissions and decay kinetics were recorded with time-gated option (90 μs delay after pulse) and at 2 Hz lamp repetition.

Even though the π-expanded–phenanthro core was essential in enhancing the lifetime of metastable ^{3}(**2**)*, this moiety was found to induce subsequent transformation of QDM **2** to form a mixture of uncharacterized products **2'**, which rendered the ^{1}H NMR signal to broaden after 24 h when kept under ambient light (Figure

3). Due to the broadening of the ^{1}H NMR, we hypothesized that **2'** is most likely constituted of persistent radicaloids. Moreover, it was possible to monitor the slow conversion of **2** to **2'** using UV-vis absorption method as depicted in Figure 3b. After complete decomposition of **2**, we attempted unsuccessfully to characterize the resulting material by NMR spectroscopy: the signals were broad and uncharacteristic of the signals of QDM **2**. We also carried out EPR experiments to corroborate the formation of persistent radical species **2'**. As shown in Figure S17, an intense EPR signal was observed after exposure of QDM **2** to light for just 2 min; from this result two conclusions can be made: a) the additional resonance energy provided by the phenanthro moiety would contribute to destabilize *ring B* in QDM **2** via rearomatization, or b) the close proximity of the sulfur atom to *ring E* would induce rearrangement or $_{Ar}$C-H insertion: (See Chart S2, Supplementary Information for the resonance structures).

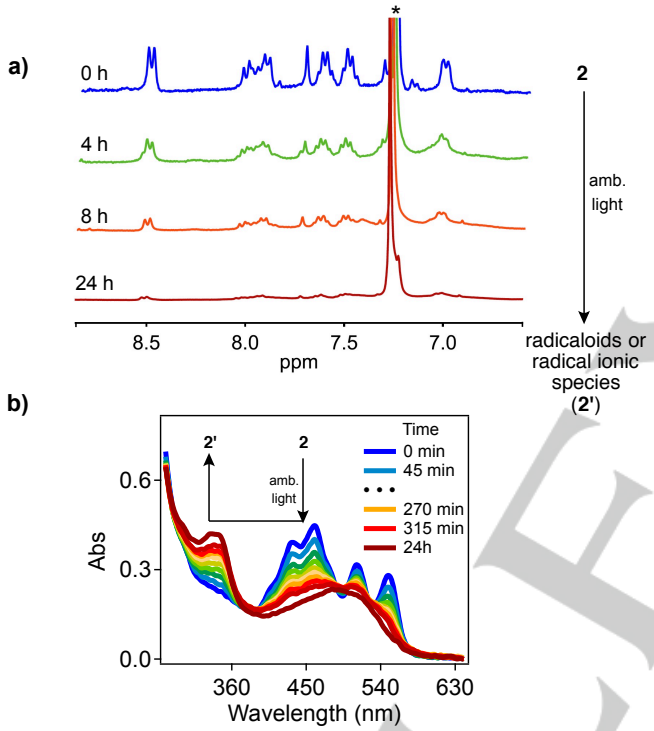

Figure 3. a) Partial ^{1}H NMR spectra of QDM **2** at various times while the NMR tube was kept at ambient conditions. b) UV-vis absorption spectra of QDM **2** recorded at various times while the sample was kept under ambient light. * residual NMR solvent peak.

Table 1. Optoelectronic Characteristics for QDM **1** and **2**.

Comp.	λ_{Abs}^{max} (nm) [a]	ε ($M^{-1}cm^{-1}$)[a]	λ_F^{max} (nm) [a]	λ_P^{max} (nm)[b]	τ_P (ms)[b],[c]	ΔE_{L-H} (eV)[d]
1	453	1631	545	725	0.4	3.18
2	460	1468	559	743	4.4	2.95

[a] UV-vis absorption and fluorescence emission. were recorded in DCM. [b] Phosphorescence was recorded in 50:50 (v/v) DCM:EtOH glass at 77 K and λ_{exc} = 470 nm. [c] Phosphorescence lifetime. [d] Calculations were performed using geometries (*N*-3-pentyl) optimized at PBE0/cc-pVTZ;[20,21] $\Delta E_{L-H} = E_{LUMO} - E_{HOMO}$.

Next, we used computational tools to assess the impact of the additional phenanthro unit on the energetics of the frontier molecular orbitals as well as on the intrinsic ground state aromaticity of the new quinoidal benzotetraphene **2**. As shown in Figure 4, the orbital pictures in the structure of QDM **2** exhibit similar features as the ones from the parent compound **1**. Although the energy levels of the orbitals have slightly increased for chromophore **2**, the HOMO-LUMO gap has shrunk from 3.18 to 2.95 eV. The decrease in electronic bandgap energy is clearly in agreement with the decrease in energy of the optical transitions as shown above in the UV-vis and emission spectroscopy results. In order to shed light on the nature of the triplet state, we also provided in Figure 4 the pictures of singly-occupied MOs (SOMOs) and the 3D spin density maps of QDM **1** and **2**. These results clearly indicate the high similarity of systems **1** and **2** in their triplet states. Altogether, we ascertain that the π-expansion has helped in narrowing the optoelectronic bandgap; on the other hand, the π-expanded–phenanthro moiety impacted the ground state global aromaticity and stability of the quinoidal benzotetraphene **2** and the corresponding thiophene **3**.

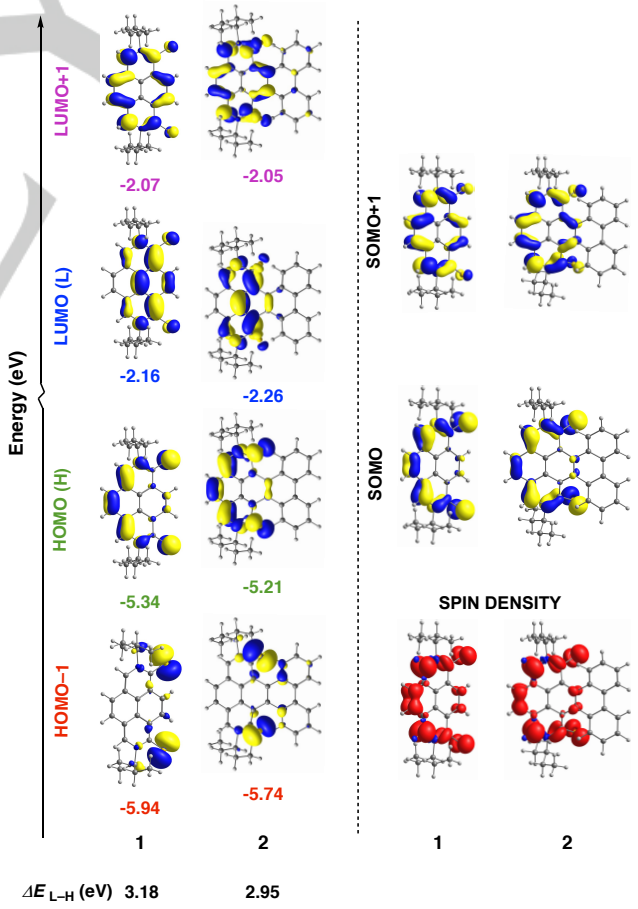

Figure 4. Frontier molecular orbital pictures and energies of QDM **1** and **2** in their singlet (*left*) and triplet (*right*) states. The latter is accompanied by

3D spin density map (isosurface 0.0035 a.u.). Calculations were performed using geometries (*N*-3-pentyl) optimized at PBE0/cc-pVTZ;[20a,21] $\Delta E_{L-H} = E_{LUMO} - E_{HOMO}$.

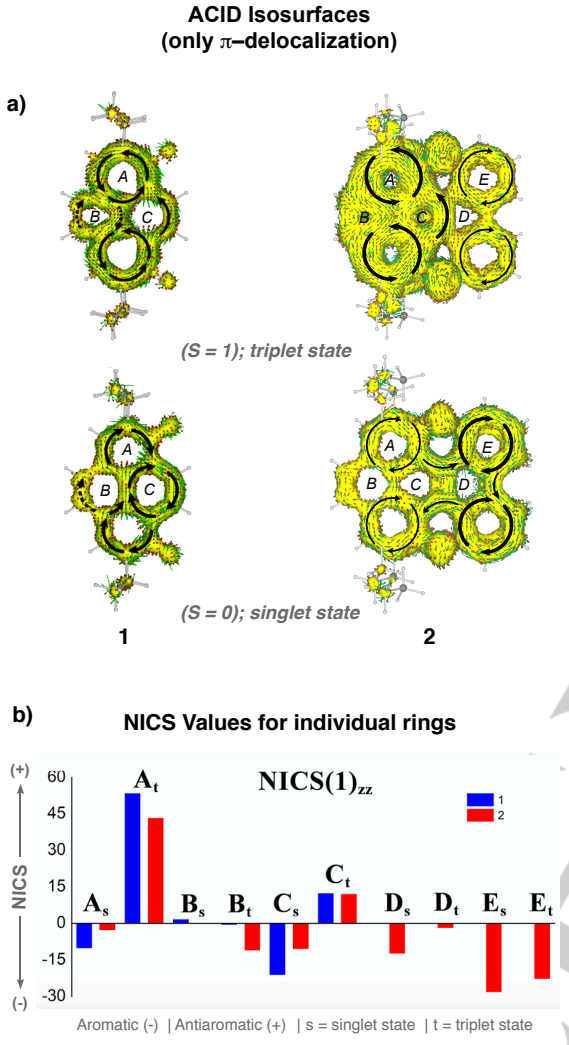

Figure 5. a) ACID[20b] isosurface plots of QDM **1** and **2** in the singlet spin state (*bottom*) and triplet spin state (*top*): iso values are 0.03 for QDM **1**, and 0.024 (singlet) and 0.0125 (triplet) for QDM **2**; current density vectors are plotted onto the ACID isosurface to indicate dia– (aromatic, clockwise) and para–tropic (anti-aromatic, counterclockwise) ring currents. Applied magnetic field direction is perpendicular to the molecular and toward outside. b) $NICS(1)_{zz}$[22,23] values for individual rings in QDM **1** and **2**: $NICS(1)_{zz}$ values are in ppm. Calculations were performed using geometries (*N*-3-pentyl) optimized at PBE0/cc-pVTZ[20a,21].

To evaluate global and local aromaticity of **2**, we performed magnetic nucleus independent chemical shift: $NICS(1)_{zz}$[22,23] calculations and ACID[20b] isosurface plots (Figure 5). As depicted in Figure 5a, besides *ring B* in QDM **1** and **2**, all other rings exhibit diatropic ring current (in the singlet state) with respect to the applied magnetic field (pointing outward), thus supporting their aromatic character. The direction of the current density vectors can be seen reversed as illustrated by the paratropic vectors (counterclockwise) once the spin state is changed (singlet → triplet). The change of tropicity of the current density vectors for the individual rings in the triplet excited state is most likely due to middle/local Baird-type aromaticity.[24] Surprisingly, *ring B* which is essentially non-aromatic, in the ground state of both QDM **1** and **2**, remains non-aromatic in ^{3}(**1**)* but this behavior is less pronounced in ^{3}(**2**)* presumably due to the decrease of aromaticity of *rings D* and *E*.

Furthermore, a closer look at the current density vectors in *ring B* revealed its low involvement into total delocalization in the singlet state (this ring could be described as essentially isolated double bond in the ground/singlet state); whereas the presence of diatropic ring current density vectors and significant delocalization are obvious in the triplet spin state for both QDM **1** and **2**. This finding agrees with spin density distribution (Figure 4 *right*), which shows delocalization of unpaired electrons in the system and significant involvement of the *ring B*. From the $NICS(1)_{zz}$ calculations for individual rings (Figure 5b and Supplementary Information, Table S2 and Figure S20), one can see that the $NICS(1)_{zz}$ values switch (from singlet to triplet excited state) except for *ring E*; however, the $NICS(1)_{zz}$ values for *rings B* indicate that these rings are notably non-aromatic in the singlet spin state while all other rings (*A, C, D*) remain aromatic for both QDM **1** and **2**. While these characteristics seemed reversed in the triplet excited state, it's still not clear whether one would label *rings B* as aromatic or non-aromatic, especially in the case of QDM **1**. Nonetheless, similar to QDM **1**, QDM **2** is globally aromatic; but, $NICS(1)_{zz}$ calculations indicate that *ring B,* which is essentially non-aromatic, gains some aromaticity characters in the triplet excited.

Conclusions

In summary, we report the synthesis of novel quinoidal benzotetraphene **2** using our previously reported quinoidization reaction from our group. The analogous thiophene system **3** was found to decompose readily upon isolation. Chromophore **2** was found to exhibit similar optoelectronic and aromaticity characteristics in comparison with parent quinoidal compound **1**. Importantly, our investigation revealed that the π-expanded–phenanthrene core was useful in producing long-lived triplet species ^{3}(**2**)* with lifetime value which is one order of magnitude higher than the triplet lifetime of ^{3}(**1**)*. But, extending the π–core has also impacted the ground state stability of **2** to generate a mixture of persistent radical species **2'**, which were responsible for the NMR signal broadening of **2**. On the basis of complementary computational results, it was found that the additional phenanthro unit contributed in the reduction of the optoelectronic bandgap. We are currently extending the quinoidization method to other less conjugated polyacene diimides to compile a library of novel triplet quinoidal acene chromophores.

Experimental Section

General Methods: All commercially obtained reagents/solvents were used as received without further purification. Unless stated otherwise, reactions were conducted in oven-dried glassware under argon atmosphere. ^{1}H-NMR and ^{13}C-NMR spectra were recorded on Bruker® 300 MHz (75 MHz for ^{13}C) spectrometer; data from the ^{1}H-NMR spectroscopy are reported as chemical shift (δ ppm) with the corresponding integration values. Coupling constants (*J*) are reported in hertz (Hz). Standard abbreviations indicating multiplicity were used as follows: s (singlet), b (broad), d (doublet), t (triplet), q (quartet), m (multiplet) and virt (virtual). Standard abbreviations in FTIR spectra were used as fellows: (st = strong, wk = weak, br = broad & sh= sharp). Data for ^{13}C NMR spectra are reported in terms of chemical shift (δ ppm). High-resolution mass spectrum data were recorded on a Bruker microTOF II or Shimadzu IT-TOF spectrometers in positive (ESI+) ion mode. UV-Vis absorption spectra were recorded on Ocean Optics® spectrometer (DH-MINI UV-VIS-NIR Light Source and QE-Pro detector using OceanView® software package). Emission spectra were recorded on an Edinburgh Instrument FLS980 spectrometer. Melting point values were recorded on a Melt-Point II® apparatus. Infra-Red spectra were recorded on PerkinElmer UATR FT-IR spectrometer. EPR experiments were performed on a Buker EMX X-band spectrometer.

Br-NDA and **Br$_2$-NDA**: A solution of dibromoisocyanuric acid (6.39 g, 22 mmol 1 equiv.) in oleum (20% SO_3, 100 mL) was added at room temperature to 500 mL oleum solution of naphthalene dianhydride **NDA** (15 g, 55.9 mmol, 0.4 equiv.) over a period of 4 h. The resulting mixture was stirred at room temperature for 1 h and then carefully poured onto ice (2 kg) to give a bright yellow precipitate. After additional 1 L of water was added to the cold solution, and the mixture was allowed to stand for overnight under stirring. The expected yellow solid was collected by suction filtration, washed with 1 N HCl solution, and dried. The crude mixture of mono- and di-brominated NDA (**Br-NDA** and **Br$_2$-NDA**) weight 16.0 g and used without further purification.

Sn-NDI: A mixture of the **Br-NDI** (3.0 g, 4.65 mmol), Bis(tributyltin) (4.71 g, 8.135 mmol, 3 equiv.) in dry toluene in the presence of $Pd_2(dba)_3$ (15 mol%) and P (*o*-tol)$_3$ (0.848, 2.79 mmol, 0.6 equiv.) under argon atmosphere was refluxed at 120 ° C for 24 h. After cooling to room temperature, the solvent was concentrated in vacuo and purified by silica gel chromatography using 1:1 DCM and Hexane. Obtained pure **Sn-NDI** as a yellow semi-solid (1.5 g, 41.2 % yield). ^{1}H NMR (300 MHz, $CDCl_3$) δ: 8.98 (s, 1H), 8.73 - 8.72 (d, *J* = 3 Hz, 2H), 4.24 - 4.19 (t, *J* = 9 Hz, 4H), 1.75 - 1.72 (m, 4H), 1.57 - 1.25 (m, 38H), 0.93 - 0.85 (m, 15H); ^{13}C NMR (75 MHz, $CDCl_3$) δ: 11.6, 13.7, 14.0, 22.6, 27.0, 27.1, 27.4, 28.0, 29.1, 29.2, 29.3, 31.8, 40.9, 41.0, 123.6, 125.9, 126.7, 130.1, 130.2, 131.6, 138.6, 156.0, 163.0, 163.1, 163.6, 164.9; ESI-HRMS: Calculated for $C_{42}H_{64}N_2O_4Sn$ [M+H] 781.3961, observed: 781.3970.

BTDI: A mixture of Sn-NDI (1.64 mmol, 1.28 g, 1 equiv.) and dibromo biphenyl (1.37 mmol, 423 mg, 0.83 equiv.) was added to round bottom flask which contains dry toluene (10 ml), and to this solution, Pd(PPh3)4 (159 mg, 0.137 mmol) and CuI (52 mg, 0.275 mmol) were added under Argonne medium then refluxed at 140 ºC for 24 h. After cooling reaction mixture to room temperature, the solvent was concentrated in vacuo and purified by silica gel chromatography using mixture of DCM and Hexane (2 : 1) as mobile phase to yield compound **BTDI**. Obtained as reddish solid (400 mg, 38 %), m.p. 117-118 ºC; 1H NMR (300 MHz, CDCl3) δ: 8.79 (s, 2H), 8.29 - 8.27 (d, J = 6 Hz, 2H), 8.16 - 8.14 (d, J = 6 Hz, 2H), 7.69 - 7.64 (t, J = 9 Hz, 2H), 7.43 - 7.38 (t, J = 9 Hz, 2H), 4.24 - 4.19 (t, J = 6 Hz, 4H), 1.78 - 1.73 (m, 4H), 1.31 - 1.25 (m, 20H), 0.89 - 0.84 (m, 6H);); 13C NMR (75 MHz, CDCl3) δ: 14.0, 22.6, 27.1, 28.1, 29.2, 29.3, 31.7, 41.4, 119.5, 123.6, 126.3, 126.4, 127.9, 130.50, 131.1, 132.5, 132.7, 140.4, 162.8, 163.3; ESI-HRMS: Calculated for C42H46N2O4 [M+H] 641.3374, observed: 641.3374.

BT-NDI: A mixture of Sn-NDI (1.64 mmol, 1.28 g, 1 equiv.) and 3,3'-Dibromo-2, 2'- bithiophene (1.37 mmol, 424 mg, 0.83 equiv.) was added to round bottom flask which contains dry toluene (10 ml), and to this solution, Pd(PPh3)4 (159 mg, 0.137 mmol) and CuI (52 mg, 0.275 mmol) were added under Argonne medium then refluxed at 140 ºC for 24 h. After cooling reaction mixture to room temperature, the solvent was concentrated in vacuo and purified by silica gel chromatography using mixture of DCM and Hexane (2 : 1) as mobile phase to yield compound **BT-NDI**. Obtained as reddish solid (400 mg, 38 %), m.p. 117-118 ºC; 1H NMR (300 MHz, CDCl3) δ: 8.77 - 8.74 (d, J = 3 Hz, 2H), 7.27 - 7.25 (d, J = 6 Hz, 2H), 7.14 - 7.12 (d, J = 6 Hz, 2H), 4.17 - 4.08 (m, 4H), 1.74 - 1.71 (m, 4H), 1.69 - 1.62 (m, 20H), 0.89 - 0.84 (m, 6H);); 13C NMR (75 MHz, CDCl3) δ: 14.6, 22.6, 27.0, 28.0, 29.1, 29.2, 31.7, 40.9, 111.8, 124.5, 126.8, 127.2, 128.7, 130.9, 131.0, 135.6, 142.2, 162.4, 162.8.

QDM 2: **BP-NDI** (150 mg, 0.234 mmol, 1 equiv.) and Lawesson's reagent (480 mg, 6.0 mmol, 4 equiv.) were added to anhydrous toluene (30 mL) in round-bottom flask with an attached condenser under an argon atmosphere. The mixture was stirred at reflux (140 °C) for 48 h. The resulting solution was cooled to room temperature and concentrated under reduced pressure to give a dark red-brown sticky solid. The solid was then precipitated into methanol (300 mL) and filtered to remove excess Lawesson's reagent and Lawesson's reagent byproducts. After that product was purified by silica gel chromatography using acetone and toluene (1: 100) to yield compound **2**. Obtained as reddish solid (31 mg, 22 %). 1H NMR (300 MHz, CDCl3) δ: 8.51 - 8.49 (d, J = 6 Hz, 2H), 8.04 - 7.95 (m, 4H), 7.66 - 7.59 (q, J = 6 Hz & 9 Hz , 2H), 7.53 - 7.46 (q, J = 6 Hz & 6 Hz , 2H), 7.04 - 7.00 (d, J = 6 Hz, 2H), 3.8 - 3.9 (m, 4H), 1.3 - 1.9 (m, 4H), 1.2 - 1.3 (m, 20H), 0.8 - 0.9 (m, 6H); 13C NMR (75 MHz, CDCl3) δ: 14.0, 22.6, 26.7, 26.9, 29.1, 29.2, 31.7, 55.6, 114.3, 114.5, 122.8, 124.9, 127.3, 127.6, 130.6, 130.8, 132.6, 133.1, 133.3, 159.2, 163.6. ESI-HRMS: Calculated for C42H64N2S2 [M] 643.3175, observed: 643.3175.

QDM 3: The synthetic procedure for compound **2** was adopted to prepare the thiophene analog; but, the compound decomposes during workup.

Acknowledgments

NK is thankful for the generous support as Postdoctoral Fellowship from the Center for Interdisciplinary Scientific Computation (CISC) at Illinois Tech. AYR thanks the Wrangler

Institute for Sustainable Energy (WISER) at Illinois Tech fort he generous support. This material is also based upon work supported by the National Science Foundation under a CAREER grant no. 1753012 Awarded to AJA.

Keywords: Quinoidal Acenes • Aromaticity • Anti-Aromaticity

[1] M. A. Kobaisi, S. V. Bhosale, K. Latham, A. M. Raynor, S. V. Bhosale, *Chem. Rev.* **2016**, *116*, 11685–11796.

[2] X. Zhan, T. J. Marks, M. A. Ratner, A. Facchetti, M. W. Advanced, S. Barlow, 2011, T. J. Marks, M. A. Ratner, M. R. Wasielewski, et al., *Adv. Mater. Weinheim* **2011**, *23*, 268–284.

[3] W. B. Davis, W. B. Davis, W. A. Svec, W. A. Svec, M. A. Ratner, M. A. Ratner, M. R. Wasielewski, M. W. Nature, 1998, *Nature* **1998**, *396*, 60–63.

[4] A. A. Rachford, S. Goeb, F. N. Castellano, *J. Am. Chem. Soc.* **2008**, *130*, 2766–2767.

[5] X. Chen, C. Xu, T. Wang, C. Zhou, J. Du, Z. Wang, H. Xu, T. Xie, G. Bi, J. Jiang, et al., *Angew. Chem.* **2016**, *128*, 10026–10030.

[6] S. Guo, W. Wu, H. Guo, J. Zhao, *J. Org. Chem.* **2012**, *77*, 3933–3943.

[7] O. Yushchenko, G. Licari, S. Mosquera-Vazquez, N. Sakai, S. Matile, E. Vauthey, *J. Phys. Chem. Lett.* **2015**, *6*, 2096–2100.

[8] S. Wu, F. Zhong, J. Zhao, S. Guo, W. Yang, T. Fyles, *J. Phys. Chem. A* **2015**, *119*, 4787–4799.

[9] S. Guo, J. Sun, L. Ma, W. You, P. Yang, J. Zhao, *Dyes and Pigments* **2013**, *96*, 449–458.

[10] C. Kaiser, A. Schmiedel, M. Holzapfel, C. Lambert, *J. Phys. Chem. C* **2012**, *116*, 15265–15280.

[11] D. Veldman, S. M. A. Chopin, S. C. J. Meskers, R. A. J. Janssen, *J. Phys. Chem. A* **2008**, *112*, 8617–8632.

[12] M. Abe, *Chem. Rev.* **2013**, *113*, 7011–7088.

[13] S. Shokri, M. K. Manna, G. P. Wiederrecht, D. J. Gosztola, S. Jockusch, A. Y. Rogachev, A. J.-L. Ayitou, *J. Org. Chem.* **2017**, *82*, 10167–10173.

[14] S. Shokri, G. P. Wiederrecht, D. J. Gosztola, A. J.-L. Ayitou, *J. Phys. Chem. C* **2017**, *121*, 23377–23382.

[15] C. Rémy, C. Allain, I. Leray, *Photochem. Photobiol. Sci.* **2017**, *16*, 539–546.

[16] X. Cui, C. Xiao, T. Winands, T. Koch, Y. Li, L. Zhang, N. L. Doltsinis, Z. Wang, *J. Am. Chem. Soc.* **2018**, *140*, 12175–12180.

[17] K. Nagarajan, A. R. Mallia, K. Muraleedharan, M. Hariharan, *Chem. Sci.* **2017**, *8*, 1776–1782.

[18] C. Li, C. Xiao, Y. Li, Z. Wang, *Org. Lett.* **2013**, *15*, 682–685.

[19] W. Yue, A. Lv, J. Gao, W. Jiang, L. Hao, C. Li, Y. Li, L. E. Polander, S. Barlow, W. Hu, et al., *J. Am. Chem. Soc.* **2012**, *134*, 5770–5773.

[20] a) J. Perdew, K. Burke, M. Ernzerhof, *Phys. Rev. Lett.* **1996**, *77*, 3865–3868. b) D. Geuenich, K. Hess, F. Kohler, R. Herges, *Chem. Rev.*, **2005**, *105*, 3758–3772.

[21] J. P. Perdew, K. Burke, M. Ernzerhof, *Phys. Rev. Lett.* **1997**, *78*, 1396–1396.

[22] P. V. R. Schleyer, C. Maerker, A. Dransfeld, H. Jiao, N. J. R. V. E. Hommes, *J. Am. Chem. Soc.* **1996**, *118*, 6317–6318.

[23] Z. Chen, C. S. Wannere, C. Corminboeuf, R. Puchta, P. von Ragué Schleyer, *Chem. Rev.* **2005**, *105*, 3842–3888.

[24] N. C. Baird, *J. Am. Chem. Soc.* **1972**, *94*, 4941–4948.

.

WILEY-VCH

COMMUNICATION

Entry for the Table of Contents

COMMUNICATION

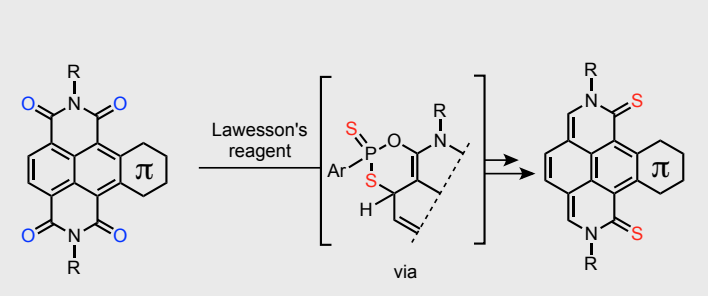

Quinoidal Acenes*

*Nareshbabu Kamatham , Jingbai Li , Siamak Shokri , Guang Yang , Steffen Jockusch, Andrey Y. Rogachev * and A. Jean-Luc Ayitou **

Page No. – Page No.

Quinoidization of π-Expanded Aromatic Diimides: Photophysics, Aromaticity, and Stability of the Novel Quinoidal Acenes

Lawesson reagent mediating quinoidization of polyaromatic acenes to afford novel quinoidal triplet chromophores